Contribution from the Department of Chemistry, The University of Texas, Austin, Texas 78712,
and The University of California, Los Alamos Scientific Laboratory, Los Alamos, New Mexico 87545

Fourier Transform Carbon-13 Magnetic Resonance of Aqueous Nickel(II)-Acetic Acid Solutions. II. Ligand Substitution Processes[1]

R. FUENTES, Jr.,[2a] L. O. MORGAN,*[2b] and N. A. MATWIYOFF

Received June 3, 1975 AIC503834

Relative abundances of monoacetatonickel(II) and bulk acetate species obtained in previous work were employed in the analysis of temperature-dependent [1-^{13}C]acetate line-broadening and chemical shift data. Slow-exchange relaxation data were analyzed using a two-term rate expression, $\tau_M^{-1} = k_{-1} + k_2 m_{Ac}$, where k_{-1} represents the acetate dissociation rate from monoacetatonickel(II), and k_2, the rate of formation of diacetatonickel(II). Calculated rate constants at 300 K, $k_{-1} = (3.9 \pm 0.3) \times 10^3$ sec^{-1} and $k_2 = (2.1 \pm 0.4) \times 10^4$ m^{-1} sec^{-1}, and activation enthalpies, $\Delta H^{\ddagger}_{-1} = 13.4 \pm 0.6$ kcal mol^{-1} and $\Delta H^{\ddagger}_2 = 12.5 \pm 0.5$ kcal mol^{-1}, are consistent with acetate exchange controlled by loss of acetate and water, respectively, from $Ni(H_2O)_5Ac^+$. In the latter case, loss of water is followed by acetate entry and subsequent rapid dissociation of the diacetato species. No dependence of either dissociation rate upon ionic strength was observed in the range 1–4 m and from 0 to 14°C. The apparent nickel(II) [1-^{13}C]acetate hyperfine coupling constant increases roughly with ionic strength: $A/h = 3.0 \times 10^5$ to 3.5×10^5 sec^{-1}, from $I = 1.2$ to 4.0. Dipole–dipole interaction dominates carbon-13 transverse nuclear relaxation for [1-^{13}C]acetate bound to nickel(II).

Introduction

Ligand-exchange processes and complex formation reactions in aqueous solutions of nickel(II) and nitrogen and/or oxygen donor ligands have been investigated extensively.[3-10] Chemical relaxation methods[11] have provided a large portion of the kinetic information for such reactions. Because of the experimental conditions required by these relaxation methods,[11] a great deal of the kinetic data has been obtained at 0.1–0.2 M ionic strength. A few NMR experiments have been done to explore the effects of high salt concentrations on metal–ligand exchange rates with varied results and conclusions.[12-17] The latter investigations have employed high ligand concentrations relative to metal ion, so that interpretation of the relaxation and chemical shift data could be done in terms of solutions dilute in paramagnetic ion.[18]

Relative abundances and equilibrium quotients for monoacetatonickel(II), $Ni(H_2O)_5Ac^+$, in nickel(II)–[1-^{13}C]acetic acid aqueous solutions over a 3 m range of ionic strength, were previously reported.[19] Those values were obtained by integration of the spectral peaks attributable to distinct coordinated and bulk 90 atom % ^{13}C-carboxyl-labeled acetate signals and are used in the present paper in the analysis of line-broadening and chemical shift data. High relative abundances of bound species preclude direct application of the Swift and Connick approximations[18] to the complete temperature dependence of the paramagnetic line-broadening and chemical shift data. However, treatment of the low-temperature relaxation data is relatively straightforward in the slow-exchange limit for the case of chemical exchange between two sites of comparable population.[20] Slow-exchange results reported here are most appropriately analyzed by means of a two-term rate expression containing an acetate-independent and an acetate-dependent exchange term. The latter provides a possible explanation for the high-temperature shift results, which do not follow Curie behavior for a single acetate species. Direct observation of the chemical shift allows evaluation of parameters describing ^{13}C transverse nuclear relaxation processes in the primary coordination sphere of the paramagnetic nickel(II) ion.

Experimental Section

Nickel(II) perchlorate–[1-^{13}C]acetic acid solutions in 99.5% D_2O were prepared by weight as discussed previously.[19] Concentrations of all solutions are given in molal (m) units. Fourier transform ^{13}C magnetic resonance measurements were made as before[19] on a Varian XL-100-FT-15 spectrometer operating at 25.2 MHz. Transverse relaxation rates, T_2^{-1}, were measured from the full line width at half-maximum peak intensity, $\Delta\nu$, according to $T_2^{-1} = \pi\Delta\nu$. Relaxation rates, T_{2A}^{-1}, for [1-^{13}C]acetate in the absence of nickel(II) were found to be negligible ($\sim$5 sec^{-1}) relative to T_2^{-1} so that $T_{2P}^{-1} = T_2^{-1} - T_{2A}^{-1} \cong T_2^{-1}$. Accuracy and reproducibility of T_2^{-1} were ±10%, or better. Carbon-13 chemical shifts were reported in ppm upfield from the carboxylate carbon resonance of acetate ion in the absence of nickel(II) ion. [1-^{13}C]Acetate in D_2O, at the same pH as, and the approximate ionic strength (by addition of $NaClO_4$) of the solution under investigation, was used as an external reference. Bulk susceptibility corrections were found to be of the same order ($\sim$0.3 ppm) as the experimental uncertainty in the shift measurements.

Treatment of Data and Results

Bulk Acetate Relaxation. Values of T_{2P}^{-1}, the relaxation rates due to nickel(II), are given in Table I as a function of temperature, and solution compositions are given in Table II. Representative spectra as a function of temperature are shown in Figure 1. Separate bound and bulk acetate ^{13}C signals are seen to overlap and coalesce above 20°C.

In the limit of slow exchange and for the case of well-resolved bound and bulk NMR signals, T_{2P}^{-1} is given by[20,21]

$$T_{2P}^{-1} = P_M P_L^{-1} \tau_M^{-1} \tag{1}$$

where τ_M is the lifetime of coordinated ligand in the first coordination sphere of the metal ion. P_M and P_L are the respective mole fractions of bound and bulk ligand.

Using the known species distribution, τ_M^{-1} (sec^{-1}) for individual solutions was calculated from eq 1 at a series of temperatures. Rate ($=\tau_M^{-1}$) vs. acetate concentration (m) profiles were obtained at 0, 3, 6, 11, and 14°C, as shown in Figure 2. In some cases, where the required data were not available at the specified temperatures, interpolated values for τ_M^{-1} were obtained by fitting the observed line broadening to eq 1 by a nonlinear least-squares procedure.[22]

Linear least-squares lines obtained for the rate profiles in Figure 2 gave positive nonzero intercepts, suggesting a two-term rate expression of the form

$$k_{ex}(=\tau_M^{-1}) = k_{-1} + k_2 m_{Ac} \tag{2}$$

where k_{-1} (sec^{-1}) is an acetate-independent term representing the acetate dissociation rate for monoacetatonickel(II), $Ni(H_2O)_5Ac^+$, k_2 (m^{-1} sec^{-1}) is an acetate-dependent term, and k_{ex} (sec^{-1}) is the total observed rate of acetate exchange obtained from eq 1. Deviations from linearity at the higher acetate concentrations ($m_{Ac} > 0.6$) for the 11 and 14°C profiles indicate that eq 1 no longer adequately represents the observed line broadening. Preliminary calculations for that region showed that the fast-exchange term for line broadening,[18,20,23] $\tau_M \Delta\omega_M^2$, contributes almost 10% to the observed

Table I. Carbon-13 Line Broadening and Chemical Shifts for Nickel(II)–[1-^{13}C]Acetic Acid Aqueous Solutions

T, °C	T_{2p}^{-1}, sec^{-1}	$(T_2^{-1})_B$, sec^{-1}	$\Delta\omega$, ppm	$\Delta\omega_M$, ppm
		Solution A		
−5	207	1300	1.0	106.3
3	384	1900	1.3	103.1
6	460		1.8	101.6
10	613		2.3	100.5
14	767		3.0	
21.5	1000		4.6	
26	1100		8.4	
32	1000		12.5	
38	900		14.3	
43	633		16.0	
51.5	460		17.0	
56	345		18.3	
61.5	280		19.2	
67	237		19.9	
72	210		20.9	
		Solution B		
−4.5	324	1800	0.1	108.5
−2	386	2000	0.9	107.5
3	565	2100	1.3	106.3
5.5	652		1.8	103.6
11	900		2.5	102.0
16	1150		4.4	
23	1740		9.7	
29.5	1880		12.8	
35	1750		16.4	
42	1270		20.5	
46.5	1070		23.1	
52	743		24.8	
57	598		26.6	
62.5	500		27.2	
67.5	410		29.0	
72.5	361		30.2	
77.5	318		31.7	
83	275		32.9	
89	235		34.0	
		Solution C		
−1.5	383	1070	0.5	111.0
0	450	1190	0.6	110.0
3	565	1370	0.7	109.4
7	767	1740	1.0	108.0
11	1010	2150	1.5	105.4
17	1900		3.0	103.2
		Solution D		
1	586	1600	0.7	111.2
6	880	2000	1.0	109.5
10.5	1270	2450	2.0	106.5
17	1990	3500	3.5	104.8
21	2800		6.4	
		Solution E		
3	830	2000	0.7	109.5
5	900	2200	1.2	109.1
6	1060	2400	1.4	108.3
8	1300	2850	3.1	107.9
14	2220	4000	5.0	105.2
17	2450	5000	7.0	104.2
		Solution F		
−8	324	1320	0.5	112.4
0	630	2150	1.1	110.9
2	824	2400	1.6	110.5
5	1000	2680	2.1	108.7
10	1400	3400	3.7	106.0
11	1500	3500	4.7	105.7
14	1900	3800	6.3	105.1
23	2650		13.4	
30	2380		18.6	
37	1690		27.9	
42	1190		31.7	
47	960		34.1	
51	805		35.7	
66	479		40.0	
79	384		44.0	
		Solution G		
0	720	1400	0.6	111.3
3	920	1720	0.8	110.1
8.5	1400	2450	1.5	108.5
14	2530	3500	1.8	105.3
19.5	3960	5000	5.7	103.5
25	4870		22.5	
31	4520		36.7	
36.5	3310		43.9	
41	2300		45.7	
46.5	1760		49.1	
52	1190		51.1	
57	920		53.0	
		Solution H		
−1	650	1400	0.1	113.3
3	1000	1800	0.5	111.5
6	1240	2100	0.8	109.5
14	2400	3100	1.0	107.1
25	5340		5.4	
31	4890		49.0	
36	3950		53.1	
40	2920		54.0	
46.5	2310		56.3	
52	2080		60.8	
57	1660		63.5	
62.5	1450		66.8	
67.5	1230		69.9	
		Solution I		
−1.5	652	1750	0.6	113.0
0	729	1920	0.7	112.1
3	1000	2340	1.0	111.1
5.5	1300	2700	1.3	110.1
11	1900	3100	2.3	108.0
21.5	2990		7.0	
29	2690		29.9	
36.5	2110		35.4	
43	1540		37.6	
51.5	1210		40.8	
57	978		42.3	
61.5	900		43.7	
67	767		45.1	
72	690		46.4	
		Solution J		
−5	424	1120	0.0	119.6
−2.5	502	1230	0.0	118.3
0	650	1400	0.1	117.0
2.5	825	1610	0.3	115.9
5	920	1750	0.6	115.4
7	1230	2140	0.8	114.5
9	1380	2380	1.6	113.9
12	1580	2900	2.1	112.7
		Solution K		
−1.5	615	1190	0.0	121.5
3	860	1460	0.2	119.4
4.5	920	1530	0.4	119.0
8	1230	1880	0.6	117.0
15.5	2000	2770	1.8	114.5
		Solution L		
−6	530	1480	0.0	123.0
−1	805	1960	0.3	120.0
1	995	2200	0.6	119.2
3	1070	2450	1.0	119.0
5	1270	2870	1.3	119.0
6	1360	3040	1.7	117.1
7.5	1610	3450	2.0	116.1
12.5	2260	4200	4.0	113.5
25	4210		24.1	
30.5	3300		35.9	
37	2450		40.5	
44	1990		42.6	
48	1860		44.0	
56	1530		45.0	
67	1270		48.0	
76	1230		48.0	

Table II. Solution Compositions and Scalar Coupling Constants for Nickel(II)–[1-^{13}C]Acetic Acid Aqueous Solutions

Soln	$(m_{\mathrm{Ni}})_0$	$(m_{\mathrm{HAc}})_0$	m_{Ac^-}	I, m	P_{M}	$10^{-5}A/h$, sec^{-1}
A	0.192	0.988	0.835	1.24	0.11_5	3.0
B	0.258	0.866	0.689	1.25	0.16_5	3.1
C	0.466	0.238	0.143	1.41	0.36	3.2
D	0.472	0.504	0.320	1.50	0.31	3.2
E	0.500	0.584	0.355	1.58	0.32	3.2
F	0.453	0.949	0.656	1.67	0.24	3.2
G	0.701	0.552	0.310	2.09	0.39	3.2
H	0.841	0.451	0.217	2.45	0.43	3.3
I	0.458	0.969	0.569	2.89	0.28_5	3.3
J	0.472	0.500	0.270	3.00	0.36	3.4
K	0.460	0.238	0.107	3.21	0.46	3.5
L	0.456	0.965	0.455	4.04	0.34	3.5

line widths. Data representing rates greater than 6000 sec^{-1} and $m_{\mathrm{Ac}} > 0.6$ were therefore omitted from consideration for 11 and 14°C. Results of linear least-squares analysis are given in Table III and displayed in Figure 3.

Table III. Linear Least-Squares Results from Acetate Concentration vs. Rate Profiles

T, °C	k_{-1}, sec^{-1}	k_2, m^{-1} sec^{-1}	T, °C	k_{-1}, sec^{-1}	k_2, m^{-1} sec^{-1}
0	415	2560	11	1140	6110
3	530	3420	14	1350	8180
6	720	4430			

Table IV. Exchange Activation Parameters for Nickel(II)–[1-^{13}C]Acetic Acid Aqueous Solutions

Process	$\Delta H^{\ddagger}$, kcal/mol	$\Delta S^{\ddagger}$, eu	Rate const at 300 K
k_{-1}	13.4 ± 0.6	2 ± 2	$(3.9 \pm 0.3) \times 10^3$ sec^{-1}
k_2	12.5 ± 0.5	3 ± 2	$(2.1 \pm 0.4) \times 10^4$ m^{-1} sec^{-1}

Acetate exchange activation enthalpies, $\Delta H^{\ddagger}$, and activation entropies, $\Delta S^{\ddagger}$, were obtained in the usual way. The activation entropy $\Delta S^{\ddagger}_2$ is referenced to the standard state of a hypothetical 1 m solution of $Ni(H_2O)_5Ac^+$.[24,25] Quantities thus obtained are given in Table IV, including the exchange rates

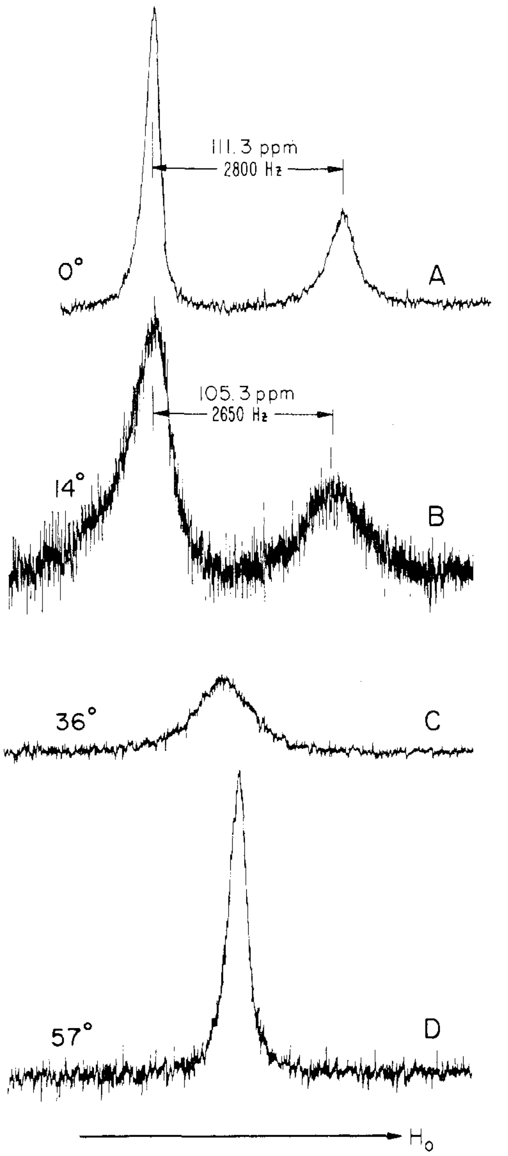

Figure 1. The 25.2-MHz ^{13}C NMR spectra of solution G at a series of temperatures. The bulk acetate and monoacetatonickel(II) resonances appear downfield and upfield, respectively, in A and B.

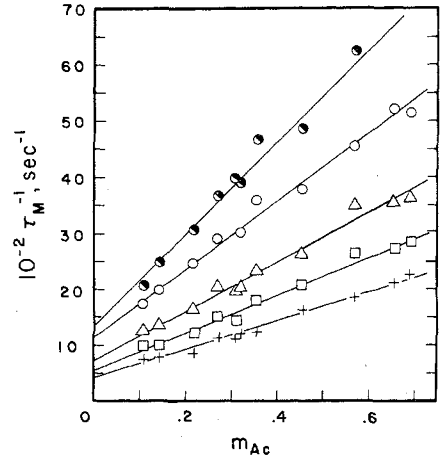

Figure 2. Acetate-exchange rate vs. free acetate concentration: +, 0°C; □, 3°C; △, 6°C; ○, 11°C; ◑, 14°C.

k_{-1} and k_2 at 300 K. Error limits given in Table IV are standard deviations generated by the nonlinear-least squares program.[22]

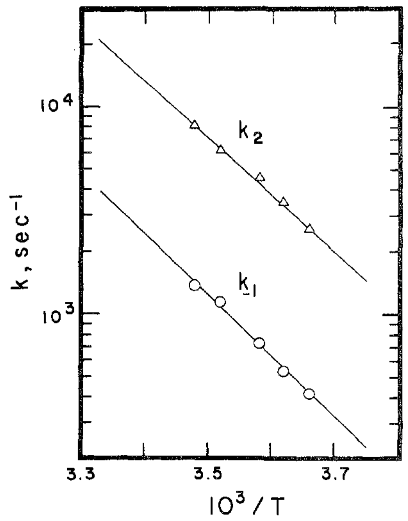

Figure 3. Temperature dependence of acetate-exchange rates k_{-1} and k_2.

Bound Acetate Measurements. Bound acetate ^{13}C shift data are given in Table I in ppm upfield from the bulk acetate resonance, i.e., as $\Delta\omega_M$ ($=\Delta\omega_{bound} - \Delta\omega_{bulk}$). Values for A/h (sec^{-1}), the nuclear–electronic hyperfine coupling constant for [1-^{13}C]acetate, were obtained from the $\Delta\omega_M$ values given in Table I according to[26]

$$A/h = \frac{3kT}{2\pi}\,\frac{\Delta\omega_M}{\omega_I}\,\frac{\gamma_I}{S(S+1)g_{eff}\beta} \qquad (3)$$

Here $g_{eff}\beta$ and γ_I are the magnetogyric ratios of the unpaired nickel(II) electrons and the ^{13}C nucleus, respectively, ω_I is the precessional frequency of the ^{13}C nucleus, S is the electron spin quantum number, k is the Boltzmann constant, and T is the absolute temperature. Calculation of A/h from eq 3 depends on the effective g value for the electron. The effective isotropic g value of 2.25 obtained from electron spin resonance measurements on hydrated nickel(II) salts[27] is consistent with that observed for the solution species in aqueous $NiCl_2$ by Evans[28a] and in a variety of aqueous nickel(II) salts containing potential carboxylate ligands over a wide range of concentrations (Gouy balance) in this laboratory.[28b] Evaluation of A/h for individual solutions showed the scalar coupling constant to be temperature independent over the temperature range −5 to +20°. Values for A/h are listed in Table II.

In the limit of slow chemical exchange and large chemical shift, the bound acetate line width, $(T_2^{-1})_B$, can be shown to be[20]

$$(T_2^{-1})_B = T_{2M}^{-1} + \tau_M^{-1} \qquad (4)$$

where T_{2M} is the intrinsic relaxation time for [1-^{13}C]acetate nuclei in the first coordination sphere of nickel(II). Line broadening, $(T_2^{-1})_B$, should increase with increasing temperature if τ_M^{-1} is the dominant contributor, and this is verified experimentally. To obtain T_{2M}^{-1} it is necessary to subtract τ_M^{-1} (known from the bulk acetate relaxation analysis) from the observed bound acetate resonance line widths, which are listed in Table I. It is expected that temperature dependence of the nuclear relaxation process is given by

$$T_{2M}^{-1} = (T_{2M}^{-1})_0 \exp(-E_M/RT) \qquad (5)$$

where $(T_{2M}^{-1})_0$ is the relaxation rate at 300 K and E_M is the energy barrier for transverse nuclear relaxation. Some scatter was observed for the resolved estimates of T_{2M}^{-1} obtained from eq 4, but the average values $(T_{2M}^{-1})_0$ = 300 ± 100 sec^{-1} and E_M = −2.0 ± 1.0 kcal/mol adequately represent the majority of the data.

Carbon-13 ($I = 1/2$) nuclear relaxation caused by the nickel(II) ion is expected to be the sum of dipole–dipole (DD) and Fermi contact (HF) interactions

$$T_{2M}^{-1} = DD + HF \tag{6}$$

The dipolar contribution for the conditions obtaining in these experiments, $\tau_c^{-1} > \omega_s$ and τ_s^{-1} large, so that $\tau_s^{-1} = \tau_c^{-1}$, is given by[29]

$$DD = \left(\frac{4}{3}\right)\frac{S(S+1)}{r^6}(g_{\text{eff}}\beta)^2\gamma_I^2\tau_s \tag{7}$$

where r is the electronic–nuclear distance, τ_c is the effective correlation time for the dipolar electron spin–nuclear spin interaction, τ_s is the electronic relaxation time, ω_s is the electron Larmor precessional frequency, and other symbols are as previously defined.

The Fermi contact, or hyperfine, relaxation term, for the conditions $\tau_e^{-1} \gg \omega_s$ and large τ_s^{-1} so that $\tau_s^{-1} = \tau_e^{-1}$, is given by[29]

$$HF = \frac{S(S+1)}{3}\left(\frac{A}{\hbar}\right)^2\tau_s \tag{8}$$

where τ_e is the effective correlation time for isotropic nuclear–electronic spin exchange, and $A/\hbar$ is in rads per second.

Acetate Chemical Shifts Chemical shift data for [1-^{13}C]acetate are given in Table I in ppm upfield relative to external [1-^{13}C]acetate. As shown in Figure 1, distinct bound and bulk acetate resonances are observed below 20°C. Single-peak NMR spectra are observed at temperatures greater than 20°C, although incomplete averaging appears to occur between 20 and 40°C. Completely averaged spectra are observed above 40°C. The observed upfield shift, $\Delta\omega$, from free acetate in the absence of nickel(II) continues to increase with increasing temperature for all solutions investigated. That is, the high-temperature shifts do not obey the chemical shift expression in the fast-exchange limit for the single-complex model

$$\Delta\omega = P_L\Delta\omega_L + P_M\Delta\omega_M \tag{9}$$

where $\Delta\omega_M$ and $\Delta\omega_L$ are the chemical shifts for bound and bulk acetate, respectively. Since $\Delta\omega_M \gg \Delta\omega_L$ for the present conditions, eq 9 reduces to

$$\Delta\omega = P_M\Delta\omega_M \tag{10}$$

Calculation of the expected chemical shift, $\Delta\omega_{\text{calcd}}$ at high temperature from eq 10 for each individual solution was performed using the $\Delta\omega_M$ values given in Table I, assuming the temperature dependence of the chemical shift to be given by

$$\Delta\omega_M = (\Delta\omega_M)_0/T \tag{11}$$

where $(\Delta\omega_M)_0$ is the chemical shift at 300 K. Residual or excess shifts, defined as

$$\Delta\omega_R = \Delta\omega - \Delta\omega_{\text{calcd}} \tag{12}$$

were plotted vs. $1/T$, resulting in residual shift slopes of 4–6 kcal/mol for all solutions analyzed. A typical example is shown in Figure 4. Assuming the residual shifts to be attributable to formation of higher species and/or conformational changes, the residual shift slopes may represent the enthalpy of formation for diacetatonickel(II) or, perhaps, the enthalpy required for configurational conversion.

Discussion

Analysis of the relaxation data in the limit of slow exchange is self-consistent. The acetate-dependent term in the rate expression may arise most plausibly from (a) associative acetate displacement through a seven-coordinate intermediate, (b) proton transfer from a coordinated water molecule to free acetate, which is expected to labilize the nickel(II) inner coordination sphere,[4,5] or (c) rapid equilibrium formation of diacetatonickel(II), $Ni(H_2O)_xAc_2$. Very few, if any, clear-cut examples of process (a) have been found for octahedral complex substitution,[30,31] so that an associative mechanism based on a long-lived (relative to diffusion-controlled ligand exchange between the outer sphere[32] and the bulk solution)[25] seven-coordinate intermediate is not favored.

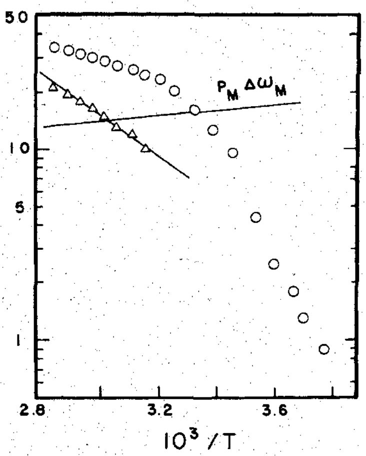

Figure 4. Temperature dependence of ^{13}C shifts of solution B: ○, observed shift $\Delta\omega$; △, residual shift $\Delta\omega_R$. Residual shift slope is 4.6 kcal/mol.

Process (b) is analogous to the internal conjugate base mechanism proposed by Rorabacher.[33,34] A coordinated water molecule could conceivably form a hydrogen bond or completely transfer a proton to an acetate ion in an outer-sphere position. In effect, this imparts partial, or full, hydroxide character to that particular water molecule. Hydroxide ion in the inner sphere is presumed to enhance the rate of water exchange relative to that for the corresponding hexaaquometal ion species on the basis of the observed behavior of a number of trivalent ions and copper(II).[35] Enhancement of the water-exchange rate was observed directly in the case of iron(III),[36,37] where that for $Fe(H_2O)OH^{2+}$ was a factor of 100 greater than for $Fe(H_2O)_6^{3+}$.

Similar arguments, in terms of a labilized inner sphere, may be made for process (c). The presence of a monodentate anion in the inner coordination sphere of a metal ion has been shown to enhance the rate of water exchange, presumably because of changes in electron density caused by metal–ligand bond formation.[4,5] However, negatively charged carboxylate groups, in general, only slightly enhance the lability of water molecules.[38,39]

Reported values for k_{-1}, the acetate dissociation rate for $NiAc^+$, are 5×10^3 sec^{-1} from T-jump relaxation[40,41] and 4.5×10^3 M^{-1} sec^{-1} from a spectrophotometric method.[42] These are in excellent agreement with the value obtained here, $k_{-1} = 3.9 \times 10^3$ sec^{-1}, considering that experimental conditions are vastly different. Ascribing k_2, the acetate-dependent rate, to the forward rate of diacetatonickel(II) complex formation is consistent with a formation rate determined by the water-leaving rate from $NiAc^+$. If complex formation proceeds as

$$\begin{gathered} Ni(H_2O)_6^{2+} + Ac^- \underset{k_{-1}}{\overset{k_1}{\rightleftharpoons}} Ni(H_2O)_5Ac^+ + H_2O \\ Ni(H_2O)_5Ac^+ + Ac^- \underset{k_{-2}}{\overset{k_2}{\rightleftharpoons}} Ni(H_2O)_xAc_2 + (5-x)H_2O \end{gathered} \tag{13}$$

then k_2 must be less than the rate constant for dissociation of a particular water molecule from the inner sphere of Ni-

$(H_2O)_5Ac^+$ and k_{-2} is expected to be considerably greater, as a result of substitution labilization, so that Q_2, the equilibrium quotient for formation of diacetatonickel(II), and equilibrium concentrations of $NiAc_2$, should be small. The observed value for $\Delta H^{\ddagger}_2$, 12.5 kcal/mol, is appropriate for loss of H_2O from $Ni(H_2O)Ac^+$ as the rate-determining step in the formation of $Ni(H_2O)_xAc_2$.

Probable cause of the observed upfield shift for the carboxyl carbon has been discussed in some detail by Strouse et al.,[43,44] who suggested that a net negative spin density appears there as a result of spin polarization[45-47] which overwhelms the effect of direct delocalization from nickel(II) through σ orbitals. Given the same sign for the coupling constant, the direction of the shift is opposite to that expected for oxygen-17 because of the different sign of the nuclear moment in the two cases.

Observed values of the scalar coupling constant A/h appear to increase roughly with increasing ionic strength, the magnitude of the variations being much larger than the error in the shift measurement. Those variations may be attributable either to medium effects or to shift contributions from minor species. The former entail large changes in the gross ionic solution structure, and it is expected that this perturbation influences the bulk acetate resonance more strongly than that for bound acetate. As all bulk acetate shifts are referenced to external acetate at approximately the same ionic strength as that of the particular solution under investigation, medium effects have been minimized to some extent. In comparison, Hunt et al.[14] observed larger coupling constants for Ni(II)–H_2O interactions in solutions containing high LiCl or $LiClO_4$ concentrations than the values reported for more dilute solutions. However, those results were not attributed to general, or specific, salt effects because the evidence did not warrant such a distinction.[14]

Averaged shift contributions from minor species could also account for the behavior of the scalar coupling constant with respect to ionic strength. If the minor species is $Ni(H_2O)_xAc_2$, it is expected that its chemical shift will be in the same direction (to higher field) and greater than or equal to that for $NiAc^+$.[16] Exchange of acetate between $Ni(H_2O)_xAc_2$ and bulk acetate should be faster than that between $NiAc^+$ and bulk acetate assuming slight labilizing effects as discussed previously. This may be manifested as small averaged upfield shifts for the bulk acetate signal even in the slow-exchange region for $NiAc^+$ dissociation, which essentially decreases the apparent chemical shift with increased $NiAc_2$ formation and therefore also decreases the calculated A/h as $\Delta\omega_M$ becomes smaller in eq 3. Intercomplex exchange of acetate is neglected in these considerations. Interpretation of experimental results on this basis leads to the conclusion that decreased ionic strength favors formation of higher acetatonickel(II) species.

Excess chemical shift in the high-temperature, fast-exchange region also suggests the possibility of higher acetatonickel(II) species formation and/or configurational changes. On the basis of the former, analysis of the high-temperature shift data as described in a previous section leads to an estimated value of 4–6 kcal/mol for the slope of the residual shift $\Delta\omega_R$, which is attributable to the enthalpy of formation for $NiAc_2$. The formation reaction of $NiAc^+$ is assumed to have a small ΔH, on the order of 0 ± 1 kcal/mol, based on the essentially constant value of P_M over the temperature range -5 to $+20$°C for a given solution.[19] Tanaka et al.[48] also found no change in Q_1, the equilibrium quotient for formation of $Ni(H_2O)_5Ac^+$, between 15 and 35°C. No data for the formation reaction enthalpy of $NiAc_2$ are available for comparison.

Configurational change from octahedral to tetrahedral is known for chlorocobalt(II) complexes.[16] A similar configurational conversion for $Ni(H_2O)_2Ac_2$ formation could contribute to the residual shift because a tetrahedral nickel(II) complex is expected to have a scalar coupling constant 2 or 3 times greater than octahedral nickel(II). However, no independent evidence indicating tetrahedral complex formation was observed for solutions comparable to those investigated here by ^{13}C NMR.

The bound acetate measurements provide information necessary in determining the mode of ^{13}C transverse nuclear relaxation of [1-^{13}C] acetate by nickel(II). Assuming a typical value of $A/\hbar = 2.0 \times 10^6$ rads sec^{-1} for the present system and letting $\tau_e = \tau_s = 3 \times 10^{-12}$ sec for the effective correlation time for isotropic spin exchange,[49] one finds $T_{2M}^{-1} \approx 10$ sec^{-1} from eq 8. If $\tau_c = \tau_s = 3 \times 10^{-12}$ sec for the effective correlation time for dipolar relaxation and $r = 2.9$ Å from crystallographic data on solid $Ni(H_2O)_4Ac_2$,[50] then $T_{2M}^{-1} \approx 260$ sec^{-1} from eq 7. The Fermi contact interaction is seen to contribute less than 5% of the total relaxation rate, while the dipolar contribution is observed to be within the error limits of the average T_{2M}^{-1} value. Those results indicate that dipolar relaxation is the dominant mode of ^{13}C transverse nuclear relaxation for the carboxyl carbon of acetate bound to nickel(II). In comparison, dipolar relaxation is known to dominate T_{2M}^{-1} for ^1H in hexaaquonickel(II)[51] and hexaaquocobalt(II),[52] where τ_s is very short, as in the present system. The observed values of the coupling constant for the latter ions are of the same order of magnitude as those given here: $A/h = 1.1 \times 10^5$ and 3.7×10^5 sec^{-1} for protons in hexaaquonickel(II) and hexaaquocobalt(II), respectively.[51,52]

Detailed analysis of the complete temperature dependence of the ^{13}C line broadening is hampered by the small equilibrium constants for $NiAc^+$ and $NiAc_2$. Sufficient information is not available to justify such an analysis because the relaxation data appear to be a very complex function of line-broadening contributions from an unknown species distribution above the "coalescence" temperature, ~20°C. The high ionic strength employed in many of the solutions is an additional complication. Decreased water coordination seems reasonable as a result of low water activities in concentrated salt solutions, which might ultimately be the dominant factor in the observed exchange rates. Further experiments on this system by ^{17}O NMR might provide more information concerning the role of additional complex formation at higher temperatures and subsequent effects on relaxation and chemical shift data. However, the problems generated by the small formation constants of the nickel(II)–acetate system will remain regardless of the probe or method employed.

Acknowledgment. R.F. wishes to thank the Robert A. Welch Foundation for support from a graduate fellowship while at the University of Texas and the Los Alamos Scientific Laboratory, group CNC-4, for the support and courtesies extended to him during the summers of 1972, 1973, and 1974.

Registry No. $Ni(H_2O)_5Ac^+$, 25403-79-6.

References and Notes

(1) Work performed under the auspices of the USERDA and with the support of the Robert A. Welch Foundation, Houston, Tex., under Grant No. F-041.

(2) (a) Summer Research Assistant, Department of Chemistry, The University of Texas. (b) Consultant, Department of Chemistry, The University of Texas.

(3) T. R. Stengle and C. H. Langford, *Coord. Chem. Rev.*, **2**, 349 (1967).

(4) J. P. Hunt, *Coord. Chem. Rev.*, **7**, 1 (1971).

(5) D. J. Hewkin and R. H. Prince, *Coord. Chem. Rev.*, **5**, 45 (1970).

(6) K. Kustin and J. Swinehart, *Prog. Inorg. Chem.* **13**, 107 (1970).

(7) G. Nancollas, *Coord. Chem. Rev.*, **5**, 379 (1970).

(8) A. Peloso, *Coord. Chem. Rev.*, **10**, 123 (1973).

(9) M. Eigen and R. G. Wilkins, *Adv. Chem. Ser.*, **No. 49**, 55 (1965).

(10) R. G. Wilkins, *Acc. Chem. Res.*, **3**, 408 (1970).

(11) See ref 5, this work, and ref 4 therein.

(12) R. Murray, H. W. Dodgen, and J. P. Hunt, *Inorg. Chem.*, **3**, 1576 (1964).

(13) R. B. Jordan, H. W. Dodgen, and J. P. Hunt, *Inorg. Chem.*, **5**, 1906 (1966).

(14) S. F. Lincoln, F. Aprile, H. W. Dodgen, and J. P. Hunt, *Inorg. Chem.*, **7**, 929 (1968).

(15) A. H. Zeltmann and L. O. Morgan, *J. Phys. Chem.*, **70**, 2807 (1966).
(16) A. H. Zeltmann, N. A. Matwiyoff, and L. O. Morgan, *J. Phys. Chem.*, **72**, 121 (1968); **73**, 2689 (1969).
(17) A. H. Zeltmann and L. O. Morgan, *Inorg. Chem.*, **10**, 2739 (1971).
(18) T. J. Swift and R. E. Connick, *J. Chem. Phys.*, **37**, 307 (1962).
(19) R. Fuentes, Jr., L. O. Morgan, and N. A. Matwiyoff, *Inorg. Chem.*, **14**, 1837 (1975).
(20) T. J. Swift in "NMR of Paramagnetic Molecules", G. N. La Mar, W. DeW. Horrocks, Jr., and R. H. Holm, Ed., 1st ed, Academic Press, New York, N.Y., 1973, Chapter 2.
(21) T. J. Swift and G. P. Weinberger, *J. Am. Chem. Soc.*, **90**, 2023 (1968).
(22) R. H. Moore and R. K. Zeigler, Report LA-2367, Los Alamos Scientific Laboratory, Los Alamos, N.M., Oct 1959.
(23) J. Granot and D. Fiat, *J. Magn. Reson.*, **15**, 540 (1974).
(24) S. Rasmussen, *Acta Chem. Scand.*, **10**, 1279 (1956).
(25) T. W. Swaddle, *Coord. Chem. Rev.*, **14**, 217 (1974).
(26) N. Bloembergen, *J. Chem. Phys.*, **27**, 595 (1957).
(27) K. H. Hellwege and A. M. Hellwege, Ed., "Magnetic Properties of Transition Metal Compounds", Springer-Verlag, New York, N.Y., 1966.
(28) (a) D. F. Evans, *J. Chem. Soc.*, 2003 (1959); (b) L. A. Meiske, unpublished results.
(29) A. Abragam, "Principles of Nuclear Magnetism", Oxford University Press, London, 1961, Chapter 8.
(30) R. G. Pearson, D. N. Edgington, and F. Basolo, *J. Am. Chem. Soc.*, **84**, 3233 (1962).
(31) M. L. Tobe, *Rec. Chem. Prog.*, **27**, 79 (1966).
(32) M. Eigen in "Advances in the Chemistry of the Coordination Compounds", S. Kirschner, Ed., Macmillan, New York, N.Y., 1961, p 371.
(33) D. B. Rorabacher, *Inorg. Chem.*, **5**, 1891 (1966).
(34) R. N. Taylor, H. K. Stepien, and D. B. Rorabacher, *Inorg. Chem.*, **13**, 1282 (1974).
(35) See ref 33, this work, and ref 21–24 therein.
(36) R. E. Connick and E. D. Stover, *J. Phys. Chem.*, **65**, 2075 (1961).
(37) E. E. Genser, Ph.D. Thesis, University of California, Berkeley, Calif., 1962.
(38) D. W. Margerum and H. M. Rosen, *J. Am. Chem. Soc.*, **89**, 1088 (1967).
(39) J. P. Jones, E. J. Billo, and D. W. Margerum, *J. Am. Chem. Soc.*, **92**, 1875 (1970).
(40) H. Hoffmann, *Ber. Bunsenges. Phys. Chem.*, **73**, 432 (1969).
(41) H. Hoffmann and E. Yeager, *Ber. Bunsenges. Phys. Chem.*, **74**, 641 (1970).
(42) S. Funahashi and M. Tanaka, *Inorg. Chem.*, **8**, 2159 (1969).
(43) C. E. Strouse and N. A. Matwiyoff, *Chem. Commun.*, 439 (1970).
(44) N. A. Matwiyoff, C. E. Strouse, and L. O. Morgan, *J. Am. Chem. Soc.*, **92**, 5222 (1970).
(45) H. M. McConnell and D. B. Chestnut, *J. Chem. Phys.*, **28**, 107 (1958).
(46) J. A. Culpa and R. De Boer, *Mol. Phys.*, **7**, 333 (1964), and references therein.
(47) D. Ladzius and M. Karplus, *J. Chem. Phys.*, **44**, 1600 (1966), and references therein.
(48) N. Tanaka and K. Kato, *Bull. Chem. Soc. Jpn.*, **32**, 516 (1959); N. Tanaka, Y. Saito, and H. Ogino, *ibid.*, **36**, 794 (1963).
(49) N. Bloembergen and L. O. Morgan, *J. Chem. Phys.*, **34**, 842 (1961).
(50) J. K. Van Niekerk and R. F. L. Schoenig, *Acta Crystallogr.*, **6**, 609 (1953).
(51) B. B. Wayland and W. L. Rice, *Inorg. Chem.*, **5**, 54 (1966).
(52) N. A. Matwiyoff and P. E. Darley, *J. Phys. Chem.*, **72**, 2659 (1968).

Contribution from the Groupe d'Etude et d'Application des complexes métalliques,
Laboratoire de Chimie de Coordination du CNRS, BP 4142 31030 Toulouse Cedex, France

Dinuclear Bridged d^8 Metal Complexes. V. Preparation and Structure of $[Rh(SR)(CO)_2L]_2$ and $[Rh(SR)(CO)L]_2$ Complexes (L = Tertiary Phosphine; R = C_6H_5, *t*-C_4H_9)[1,2]

PHILIPPE KALCK and RENÉ POILBLANC*

Received March 4, 1975 AIC50164I

Addition of a tertiary phosphine ligand PA_3 to di-μ-phenyl-(or di-μ-*tert*-butyl-)thiolatotetracarbonyldirhodium(I) affords the pentacoordinated dinuclear rhodium complexes $[Rh(SR)(CO)_2L]_2$. NMR and infrared data are consistent with a double tetragonal-pyramidal structure, both phosphines being in the apical positions. These complexes are of low stability and lose more or less easily 2 equiv of CO giving $[Rh(SR)(CO)L]_2$. These thiolato-bridged complexes $[Rh(SR)(CO)L]_2$ have been prepared by substitution of the chloro bridges in $[RhCl(CO)L]_2$ with LiSR. Infrared and NMR data are consistent with rhodium atoms being in a square-planar environment and the structure is bent along the S–S axis. With R = *t*-Bu and with PA_3 = PMe_3, PMe_2Ph, or $P(NMe_2)_3$, a single cis isomer was found either in solution or in the solid state. However, for other prepared compounds a mixture of isomers in equilibrium was detected. The geometry of various isomers is discussed.

Introduction

Chatt and Hart[3] have shown that substitution of the chloro bridges in the complexes $Pt_2Cl_4(PA_3)_2$ by thiolato groups gives more inert derivatives toward bridge-splitting reagents. These thiolato-bridged complexes $Pt_2Cl_2(SR)_2(PA_3)_2$ exist as cis and trans isomers;[3] the more stable isomer is cis when R is aliphatic and trans when R is aromatic.

On the other hand, with dinuclear complexes of Pt(II), it is interesting to note that removing the Cl bridges by thiolato bridges modifies the structure from a planar to a bent one. Indeed in $[PtCl_2(PPr_3)]_2$[4] all atoms are coplanar while in $[PtCl(SEt)(PPr_3)]_2$[5] a dihedral angle of 130° is observed. For the dinuclear $[RhCl(CO)(PMe_2Ph)]_2$ complex a recent X-ray structural determination[1] shows a bent configuration. From the related influence of the thiolato bridges it is thus reasonable to think that for dinuclear thiolato-bridged complexes of Rh(I) the structure is still a bent one.

Previous thiolato-bridged rhodium complexes have been reported, namely, $[Rh(SR)(CO)_2]_2$[6-11] $Rh(SR)(CO)(PA_3)_2$,[8,12] $[C_8H_{12}Rh(SR)]_2$,[13] and $[Rh(SR)(P(OPh)_3)_2]_2$.[13]

In the present paper we wish to report the results of our investigations of the reactivity of $[Rh(SR)(CO)_2]_2$ complexes toward nucleophiles. The structure of the $[Rh(SR)(CO)_2PA_3]_2$ pentacoordinated complexes is described. The preparation and structure of $[Rh(SR)(CO)(PA_3)]_2$ compounds in their isomeric forms are reported.

Experimental Section

The $[RhCl(CO)_2]_2$,[14] $[Rh(SPh)(CO)_2]_2$ (**1**),[9] and $[RhCl(CO)PA_3]_2$[15] compounds were prepared as previously described.

All solvents were distilled and used under nitrogen atmosphere. Thiophenol, *tert*-butyl mercaptan, butyllithium, trimethyl phosphite, and triphenyl- and tricyclohexylphosphines were obtained from Fluka Co.; the tris(dimethylamino)phosphine was a gift from the Pierrefitte Co. The ligands $P(CH_3)_3$[16] and $P(CH_3)_2C_6H_5$[17] were prepared by published methods. Rhodium trichloride trihydrate was obtained from the "Compagnie des Métaux Précieux". Microanalyses were carried out by the "Service Central de Microanalyses du CNRS".

Infrared spectra were recorded with a Perkin-Elmer 225 grating spectrometer in hexadecane solutions or in cesium bromide pellets; in the carbonyl stretching region the spectra were calibrated by water vapor lines. Lorentz line shape analysis of the optical density of infrared curves was performed with a Du Pont 310 curve resolver. The Raman spectra were obtained in the solid state with a T 800 spectrometer equipped with an ionized argon laser (4880 Å, 1 W) from the Spectra Physics Co.

The proton magnetic studies were performed on a Varian Associates A-60A spectrometer. Dichloromethane, deuteriochloroform, benzene, and deuteriotoluene were used as solvents and tetramethylsilane as internal standard. Nuclear Overhauser experiments were carried out on a Varian Associates HA 100 spectrometer. Deuteriotoluene was